

Measurement of elastic-scattering relative differential cross sections for electron-helium collisions at low energies and small angles*

Murray M. Arnow

Department of Physics, The University of Cincinnati, Cincinnati, Ohio 45221

(Received 20 August 1973)

The experiment presented measures the relative differential cross sections in helium for the energies between 1.0 and 10.0 eV and at the angles 10°, 15°, 20°, 25°, and 30°. The results are compared to the experiments of others and are also compared to the present theories. Since experiments do not overlap very well in this region, conclusions are difficult to draw. It is easier, however, to make comparisons to the theoretical predictions. It is shown that the results of this experiment do not agree well with the theoretical predictions.

I. INTRODUCTION

The measurement of differential cross sections for electrons of energies below 10 eV when they are scattered from noble-gas targets has been done by four groups since 1931.¹⁻⁴ The data obtained from their observations have gaps in both energy and angle, and in the regions where their measurements overlap, the agreement between different experiments could be improved.

The reasons for the status of the existing data lie in the fact that the experiments were done with very-low-energy electrons. The trajectories of low-energy electrons are greatly perturbed by small electric and magnetic fields. It is not too difficult to shield out stray electric fields; it is, however, very difficult to null out all magnetic fields. In order to design an apparatus that will perform in this region, it is often necessary to consider geometrical configurations which do not allow the ability to make measurements continuously over energy and angle.

The experiment which this paper describes endeavors to make a measurement of the elastic-scattering relative differential cross section for helium in the energy range 1.0 to 10.0 eV and an angular range 10° to 30°. This experiment differs from those mentioned above in that it involves an energy region below those previously measured and an angular region closer to 0° than those previously measured.

The results of this experiment may be compared to the recent theoretical investigations of elastic scattering of electrons in helium. A problem for the investigators has been the acquisition of sufficient experimental data to confirm or refute their models. Consequently, the only method of checking their results in the areas where data are lacking has been to see whether phase shifts obtained by different methods of calculation are con-

sistent. This paper will compare the theoretical results to the experimental results.

II. APPARATUS

The scattering apparatus consisted of an electron source, an energy monochromator and accelerating grids, an atomic beam, an energy analyzer, and an electron detector (refer to Fig. 1).

The electron source (c) was the heater and cathode assembly of an RCA No. 6AU4-GTA receiving tube. The cathode was surrounded by a cylinder (cy) with a slit cut through the wall. The cathode was kept at ground potential and a potential of 50.00 V was placed on the cylinder. The current to the cylinder, depending on the cathode, ranged between 3.0 and 3.3 mA. The electrons emerged through the cylinder slit and fell on the first slit (S1) of the monochromator which was at a nominal potential of 15 V.

The monochromator consisted of two Hughes-Rojansky 127° electrostatic analyzers.⁵ Electrons entering the tandem pair of analyzers were selected so that nominally 15-eV electrons would emerge from the second analyzer. The emerging electrons would be decelerated by a uniform electric field as they passed through the grids (G1) placed at the exit slit (S2) of the analyzer. The potential on the last grid determines the energy of the electrons which bombard the gas target (volume v).

The energy analyzer was a third 127° analyzer which had a set of grids (G2) attached to the entrance slit (S3) that accelerated the electrons which were scattered from the gas target. The energy analyzer was also tuned to accept nominally 15-eV electrons. When the exit grid of the monochromator and the entrance grid of the energy analyzer were kept at the same potential, electrons whose energies were increased by the same

amount in the accelerating grids that they had lost in the decelerating grids were the only electrons that would pass through the energy analyzer. Set in this mode, the energy analyzer would accept only elastically scattered electrons. The energy analyzer could be rotated about the gas target so that elastically scattered electrons of a given direction could be studied.

Great effort was expended to make the accelerating-decelerating grids capable of altering the energy of the electron beam without affecting the trajectories of the electrons. Each grid system (G1, G2, Fig. 1) consisted of five 2-in. by 5.75-in. rectangles of No. 30 wire, supported by a frame, no part of which was closer than 2.5 in. to the electron beam. The grids were evenly spaced, and maintained at potentials linear to within 99%. In the plane of the center grid was placed a metal sheet with a 12.0×0.5 -mm slit. This slit served to define the beam while producing minimal focusing, since it coincided with the approximately plane equipotential surface near the beam. The grids and scattering region were electrostatically shielded.

The angular resolution of the analyzer was determined by looking at the straight-through electron beam and rotating the analyzer in the two directions from the center.

Six measurements of the angular spread of the straight-through beam in the energy range 3.5 to 25 eV yielded the value $0.96^\circ \pm 0.11^\circ$ for the angular full width at half-maximum (FWHM). Angular measurements of the straight-through beam are difficult, since charging effects occur (due to the high current on the analyzer) which cause variation in the readings over a time comparable to

that required to move the analyzer through the required angle. These effects make angular resolution measurements below 3.5 eV unreliable. However, as a further check on angular beam resolution, measurements were made with a slit slightly (about 0.5 mm) misaligned, and the current measured by the analyzer was found to be essentially zero for beam energies between 0 and 25 eV.

At the exit slit (S4) of the energy analyzer, a focused mesh electron multiplier (em) was inserted. The electron multiplier was shielded to prevent signals from spurious electrons. The pulses from the electron multiplier were amplified by a low-noise JFET (junction field-effect transistor) preamplifier and then amplified again in a preamplifier and discriminator. The output of the discriminator was collected and stored in a 512-channel multichannel analyzer (MCA).

The method of operation was to sweep simultaneously the exit grid of the monochromator and the entrance grid of the energy analyzer from 0.30 to 10.46 V by a voltage ramp whose non-linearity was of the order of 1 part in 10^4 . The ramp was synchronized with the MCA so that a specific channel collected pulses corresponding to a given voltage on the grids. The ramp slope and channel dwell time were chosen such that each channel had an energy width of 0.01984 eV.

After a sweep the voltage was reset to 0.30 V and the cycle restarted. A typical run consisted of 350 sweeps and took a period of approximately 18 h. The drift in settings of voltages on the analyzer and ramp was of the order of 1 part in 10^3 in an 18-h interval.

The monochromator and analyzer were operated in an evacuated bell jar. When gas was not leaked into the system, the vacuum was in the neighborhood of 10^{-8} Torr. With gas being leaked into the system the pressure was maintained at approximately 10^{-5} Torr. It was necessary to open the system to air only on the occasion of replacing the cathode. All other adjustments, such as changing the angle of the analyzer, could be done from outside the bell jar by use of special feed-throughs.

The gas-handling system consisted of a large gas reservoir connected through a vernier throttle valve. The gas then passed through a liquid-nitrogen cold trap and leaked into the vacuum system through seven 1-cm-long stainless-steel tubes whose diameters were 0.343 mm. A pressure of approximately 15 ± 1 Torr was maintained on the high-pressure side of the leak. The pressure, once set, remained at the same value for the entire run. Duplicating the pressure exactly for each run was found to be impractical. The pres-

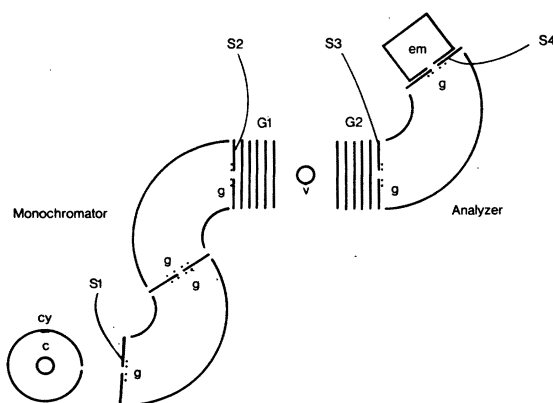


FIG. 1. Scattering apparatus: The electron source *c*; the accelerating cylinder *cy*; the collimating slits S1, S2, S3, and S4; the boundary value grids *g*; the accelerating grids G1 and G2; the target-gas volume *v*; the electron multiplier *em*.

tures were reproduced approximately, and the data were normalized by a procedure given below.

As was mentioned earlier, the magnetic fields should be reduced as much as possible. To accomplish this reduction, two sets of three rectangular wire coils were placed around the bell jar. One set was erected vertically and the other set was erected horizontally. The wire coil sets had the configuration described by Haynes and Wedding.⁶ The coils constructed produced a homogeneous field to within 0.7% for a 10-cm spherical region which contained the volume where the electrons bombarded the gas. The homogeneity was calculated from the equations given by Haynes and Wedding. The coils were positioned to align the vertical and horizontal components of the earth's magnetic field with the fields produced by the horizontal and vertical coils, respectively. Each field component was nulled at the geometric center to within 0.05 G as measured by a Hall-effect gaussmeter. The inhomogeneities in the scattering region did not exceed 0.1 G.

The energy resolution of a 127° analyzer is defined to be the FWHM, Γ , of the exiting current as a function of electron energy when the instrument is set to transmit electrons of energy E_0 . Arnov and Jones⁷ have shown that

$$\Gamma = \alpha E_0,$$

where α depends on the geometry of the entrance and exit slits and the electron source. Clearly, the best resolution is achieved if E_0 can be made very small. Practically, the lower limit for E_0 for this instrument lies about 15 eV. Using the

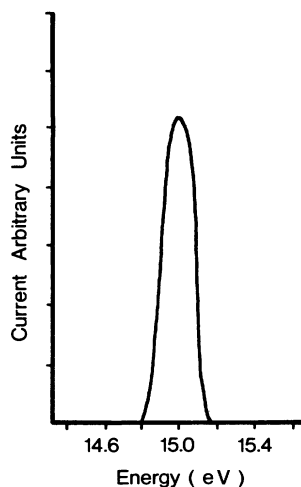


FIG. 2. Energy distribution of the transmitted current through the monochromator and analyzer when both instruments are set to pass 15-eV electrons. The FWHM is 0.2 eV.

results of Arnov and Jones, the energy resolution of the analyzer was estimated to be near 0.1 eV. It should be noted that in the quoted article, it was assumed that there were no fringing fields at the slits of the analyzer. The fringing, in practice, was minimized by placing four grid wires (g , Fig. 1) in the proximity of the slits and placing potentials on them to produce the desired boundary conditions.

The resolution of the apparatus was determined empirically by operating it in the inelastic mode; that is, by keeping the grids constant and sweeping the voltage of the analyzer slit (S3, Fig. 1) through the region of 15 V. The transmitted current is then a measure of the combined resolution of the monochromator and the analyzer and indicates a FWHM of 0.2 eV (Fig. 2).

The resolution of the monochromator was also determined by measuring the elastic resonances in N_2 near 2 eV (Fig. 3). A comparison to the experiments of Andrick and Ehrhardt⁸ and Ehrhardt and Willman⁹ showed good agreement with their results and that the above monochromator had a resolution of approximately 0.1 eV. Using the N_2 resonances, the energy scale of the apparatus could be determined to within 0.05 eV.

The angular displacement of the energy analyzer was calibrated against radial markings, known to within 0.0095°, machined on the supporting table. The analyzer was rotated by a mechanical feed-

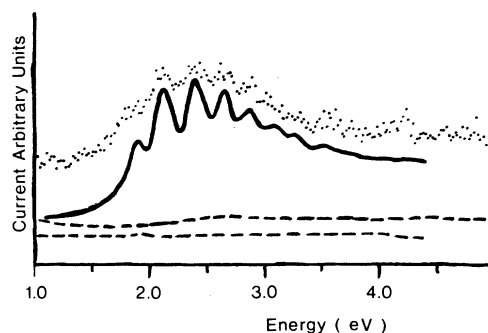


FIG. 3. Comparison of the electron current elastically scattered by N_2 as a function of incident electron energy as seen at 20° with that observed by Andrick and Ehrhardt. The two observations were normalized by adjusting the signal-minus-background electron current to be the same for the highest peak. These data were used to calibrate the nominal energy scale and resulted in a shift of 0.30 eV from the nominal value. After normalization, the signal and background curves of this work were shifted along the y axis an arbitrary amount to facilitate comparison. The curves represent raw signal data for this work (dots); signal data, Andrick and Ehrhardt (solid line); approximate background, this work (upper-dashed curve); and approximate background, Andrick and Ehrhardt (lower-dashed curve).

through which turned a lead screw which in turn moved the analyzer. By counting the rotations of the lead screw, it was possible to place the analyzer in a position known to within 0.33°

III. PROCEDURE

The procedure used was to make alternate gas and background runs at a specified angle. Each run consisted of linearly sweeping the energy of the electron beam from the nominal values 0.30 to 10.46 eV at a rate of 0.05 eV/sec. The beam was not swept from 0.00 eV because the background below 0.30 eV was too high.

Gas and background runs were made at 10° , 15° , 20° , 25° , and 30° , respectively, and were then rerun at 30° , 25° , 20° , 15° , and 10° , respectively. Two more runs were made at 10° as a check on consistency.

IV. DATA ANALYSIS

The first part of the analysis consisted of smoothing the data. This was accomplished by first converting the counts collected in each channel of the MCA into a count rate by dividing the number of counts in each channel by the total time the channel accumulated data. The 511 rates (the first channel of the MCA was not used in this experiment) were taken at energies ranging from 0.00 to 10.16 eV at increments of 0.01978 eV (the energies now quoted and henceforth stated were calibrated against the above N_2 resonances). The 511 rates were divided into consecutive groups of 11 members. Then, using the smoothing procedure suggested by Whittaker and Robinson,¹⁰ each group was least-squares fitted to a second-degree curve. The curve's value at the midpoint of the interval was used as the average of the 11 rates. Averaged in this way the 511 rates were reduced to 51 rates whose increments were

0.1978 eV, an increment more consistent with the resolution of the apparatus. The variance of each group was also computed by taking the sum of the squares of the differences of each rate from the average rate. The variance was used later in computing the errors.

The averaged rates were normalized by comparing them to a normalization run. This run consisted of measuring the rates at 10.00 eV for He and background at the five measured angles. Care was taken to make these measurements in a short time interval so that conditions would remain reasonably static. The errors for each run were estimated from the standard deviations. Each background and gas run was done twice and the rates were consistent to better than 5%. The normalization was computed from

$$\bar{R}_i(\theta, E) = [R_i^g(\theta, E) - R_i^b(\theta, E)] \times \frac{R^{ng}(\theta, 10) - R^{nb}(\theta, 10)}{R_i^g(\theta, 10) - R_i^b(\theta, 10)} \sin \theta,$$

where $\bar{R}_i(\theta, E)$ is the normalized rate at energy E and angle θ for run number i ; $R_i^g(\theta, E)$, the averaged gas rate at energy E and angle θ for run number i ; $R_i^b(\theta, E)$, the averaged background rate at energy E and angle θ for run number i ; $R^{ng}(\theta, 10)$, the normalization gas rate at 10 eV and angle θ ; $R^{nb}(\theta, 10)$, the normalization background rate at 10 eV and angle θ . The factor $\sin \theta$ was used to correct for the angular dependence of the interaction volume defined by the intersection of the incident and scattered electron beams.

Errors were computed for each rate by the method of propagation of errors; e.g., see Young.¹¹ The error computations evaluated the standard deviations which were used in obtaining the averaged rates over runs at the same angle.

The rates and rate errors computed in the above

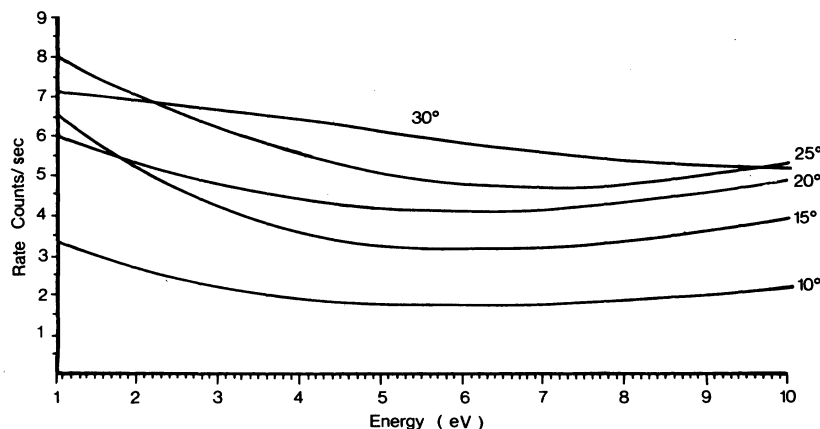


FIG. 4. Elastically scattered electron rate from a helium target as a function of incident electron energy at various angles. Care should be taken in comparing rates at different angles (see text). Typical errors in rates at a given angle are: 10° , 5%; 15° , 9%; 20° , 11%; 25° , 12%; 30° , 12%.

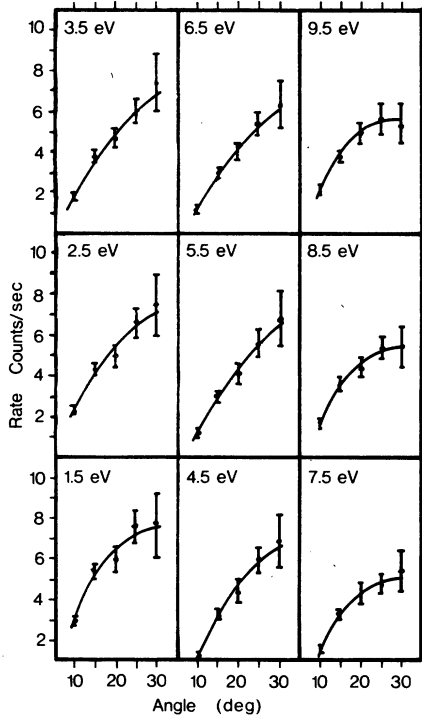


FIG. 5. Elastically scattered electron rate from a helium target as a function of angle at various incident electron energies.

fashion are actually the relative differential cross sections and their corresponding errors. Unless otherwise stated, the relative differential cross sections will be henceforth referred to as the differential cross section and symbolized by $\sigma(\theta)$.

When considering $\sigma(\theta)$ at a given angle as a function of energy, the errors are less than the errors of $\sigma(\theta)$ as a function of angle. This situation occurs because when calculating $\sigma(\theta)$ for a constant angle the calibration against the normalization runs

does nothing other than multiply the differential cross section by a constant, and the errors in that constant contribute nothing to the relative variations of $\sigma(\theta)$ as a function of energy. It is another matter when comparing the differential cross sections of varying angles; in that case the errors in the normalization constant contribute to the relative behavior of the differential cross section as a function of angle.

Cross sections below 1.00 eV are not included in this paper. The background rates below 1.00 eV were very high; thus giving a poor signal-to-noise ratio.

Figure 4 displays rate curves at constant angle as a function of energy. The rate curves were obtained by least-squares fitting the 51 data points at each angle to a second-degree polynomial. It should be emphasized that, for the reasons mentioned earlier, these curves are more meaningful if they are used to examine the $\sigma(\theta)$ as a function of energy at a given angle than if they are used to compare $\sigma(\theta)$ at constant energy as a function of angle. For example, this experiment indicates that the 30° curve is a flatter function of energy than the 25° curve, but the accuracy of comparison of the 25° and 30° curves is not sufficient to assert that the curves cross, as shown by a straightforward plotting of the data. When viewed as a function of energy, the typical standard deviations in the data points for each angle lie between 5 and 10%, the lesser errors are associated with the smaller angles.

Figure 5 displays rate curves at constant energy as a function of angle. The data for the curves were evaluated by first dividing the 51 rates at each angle into ten groups of five rates each. Each group was averaged by the use of Eq. (1) and given an energy corresponding to the midpoint energy of the group; e.g., the five rates correspond-

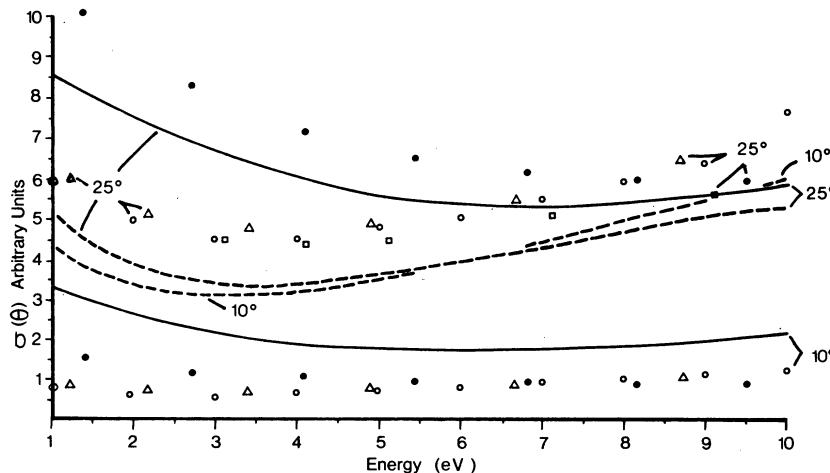


FIG. 6. Comparison of the relative differential cross sections as a function of energy between the theoretical values of Burke and Robb (●), Sinfailam and Nesbet (Δ), LaBahn and Callaway (○), the phase-shift analysis of Bransden and McDowell (dashed line), and the experimental values of Gibson and Dolder (□), and this work (solid lines).

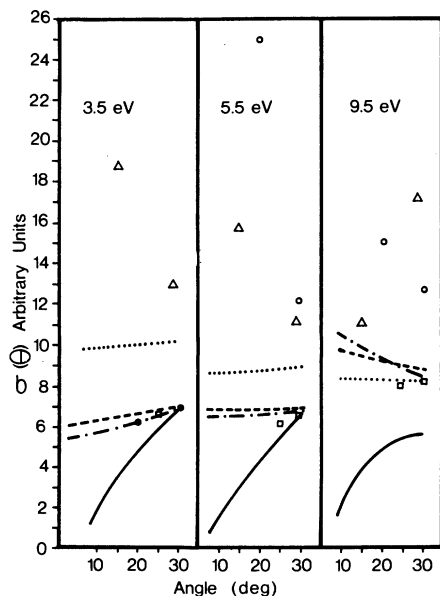


FIG. 7. Comparison of the relative differential cross sections as a function of angle between the theoretical values of Burke and Robb (dotted lines), Sinfailam and Nesbet (dashed lines), LaBahn and Callaway (dash-dot lines), and the experimental values of Bullard and Massey (\circ), Ramsauer and Kollath (Δ), Gibson and Dolder (\square), and this work (solid lines). The values of Bullard and Massey and those of this work were normalized with respect to the absolute differential cross section given by Gibson and Dolder at 3.1 eV and 30° (see text). Errors for this work are given in Fig. 5.

ing to energies 1.0–2.0 eV were averaged and the resulting rate was said to have an energy of 1.5 eV. This procedure was justified since the rates vary slowly and smoothly with energy. As was explained earlier, the errors for these rates are larger than the errors for the rates used in Fig. 4. The curves were constructed by least-squares fitting the rates at each energy to a second-degree polynomial in angle.

V. RESULTS

As was stated at the beginning of this work, experiments in this energy and angular region are sparse. The three experiments that could be compared to this investigation are those of Bullard and Massey,¹ Ramsauer and Kollath,² and Gibson and Dolder.³ The experiments are compared in part in Fig. 7. It is easily seen that agreement in the overlapping region is difficult to determine because of the paucity of data. It is therefore necessary to make most of the comparisons with the existing theories. The calculations of Burke and Robb,¹² LaBahn and Callaway,¹³ and Sinfailam and Nesbet¹⁴ are illustrated in Figs. 6 and 7. In addition, Fig. 6 includes a comparison with the

phase-shift analysis of Brandsen and McDowell.¹⁵

Figure 6 compares some of the results mentioned at 10° and 25° as a function of energy. The works compared in Fig. 6, all with the exception of this paper's results, had the differential cross sections evaluated absolutely. In order to make a comparison, the results of this paper were normalized by setting the value of the differential cross section at 25° and 9.1 eV equal to the value given by Gibson and Dolder and referring all other values to that value. It should be stated again that for reasons given earlier these curves are more meaningful if the relative change of $\sigma(\theta)$, at constant angle, as a function of energy for each research group's results are compared.

Figure 7 compares the angular dependence at constant energy of $\sigma(\theta)$. The curves in this case were normalized as with Fig. 6, except that in Fig. 7 the normalization differential cross section used was the value given by Gibson and Dolder at 3.1 eV and 30°. Bullard and Massey give relative differential cross sections, and their data were normalized by the same procedure to the latter 3.1-eV value. The energies of each quoted work lie within 1.3 eV of the energies stated in Fig. 7. This fact is not critical since the differential cross sections in all cases vary slowly and smoothly as a function of energy.

VI. CONCLUSION

The results of this work appear to agree best with theory when comparing the shape of the energy-dependence curves for $\sigma(\theta)$. The best agreement is with the curves given by Burke and Robb. The more inclusive and detailed analyses of LaBahn and Callaway and Sinfailam and Nesbet, and the phase-shift analysis of Brandsen and McDowell cannot be made to agree very well in the range of this experiment, even if the curves have different normalizations and experimental errors are considered. The comparison of the N_2 elastic resonances with the observations of others (Fig. 3) shows reasonable agreement, when allowance is made for the difference in resolution, and is an argument for confidence in the experimental curves.

The agreement of $\sigma(\theta)$ for low energies and small angles among the previous experimental workers is poor. This experiment agrees much better with the recent work of Gibson and Dolder than it does with the pioneer work of Ramsauer and Kollath, and Bullard and Massey. Gibson and Dolder have only two angular points to compare for each energy, and these points, with the exception of the 9.5 eV differential cross sections,

lie within the experimental error of this work. The theoretical investigations do not agree with the variations of $\sigma(\theta)$ as a function of angle as shown in this experiment. The variations measured are a stronger function of angle than the current theories predict, but in view of the paucity of experiments, further work in this region would be desirable.

ACKNOWLEDGMENTS

This work would not have been possible without the thoughtful help and encouragement of Professor Dale R. Jones. The author also wishes to thank the Argonne National Laboratory for the use of some electronic equipment during the course of setting up the apparatus.

*Part of a thesis submitted to the Department of Physics, The University of Cincinnati, in partial fulfillment of the requirements for the Ph.D. degree.

¹E. C. Bullard and H. S. W. Massey, Proc. R. Soc. A 133, 637 (1931).

²C. Ramsauer and R. Kollath, Ann. Phys. (Leipz.) 9, 529 (1932).

³J. R. Gibson and K. T. Dolder, J. Phys. B 2, 1180 (1969).

⁴D. Andrick and A. Bitsch, *Seventh International Conference on the Physics of Electronic and Atomic Collisions* (North-Holland, Amsterdam, 1971), p. 87. No details of the results of their measurements are given.

⁵A. L. Hughes and V. Rojansky, Phys. Rev. 34, 284 (1929).

⁶S. K. Haynes and J. W. Wedding, Rev. Sci. Instrum. 22,

97 (1951).

⁷M. Arnow and D. R. Jones, Rev. Sci. Instrum. 43, 72 (1972).

⁸D. Andrick and H. Ehrhardt, Z. Phys. 192, 99 (1966).

⁹H. Ehrhardt and K. Willman, Z. Phys. 204, 462 (1967).

¹⁰E. Whittaker and G. Robinson, *The Calculus of Observations*, 4th ed. (Blackie, London, 1924), p. 291.

¹¹H. D. Young, *Statistical Treatment of Experimental Data* (McGraw-Hill, New York, 1962), Chap. 12.

¹²P. G. Burke and W. D. Robb, J. Phys. B 5, 44 (1972).

¹³R. W. LaBahn and J. Callaway, Phys. Rev. A 2, 366 (1970).

¹⁴A. L. Sinfailam and R. K. Nesbet, Phys. Rev. A 6, 2118 (1972).

¹⁵B. H. Bransden and M. R. C. McDowell, J. Phys. B 2, 1187 (1969).